

***TSO1* functions in cell division during *Arabidopsis* flower development**

Zhongchi Liu*, Mark P. Running and Elliot M. Meyerowitz

Division of Biology, 156-29, California Institute of Technology, Pasadena, CA 91125, USA

*Author for correspondence at present address: Department of Plant Biology, University of Maryland, College Park, MD 20742-5815, USA
(e-mail: zl17@umail.umd.edu)

SUMMARY

We describe an *Arabidopsis* mutant, *tso1*, which develops callus-like tissues in place of floral organs. The *tso1* floral meristem lacks properly organized three cell layers, and the nuclei of these cells are irregular in size and shape. Further analyses reveal partially formed cell walls and increased DNA ploidy in *tso1* floral meristem cells, indicating defects in mitosis and cytokinesis. Our finding that

***TSO1* is required for organ formation in floral tissues but not in other tissues indicates that *TSO1* may encode a floral-specific cell division component, or that *TSO1* function is redundant in nonfloral tissues.**

Key word: *tso1*, mitosis, cytokinesis, floral meristem

INTRODUCTION

One of the fundamental differences between animals and plants is that plant cells are surrounded by a rigid wall, preventing cell migration. The lack of mobility of plant cells leads to the requirement for well organized and regulated cell divisions with specific cell division orientations to achieve directional growth. Like other dicots, *Arabidopsis* shoot apical meristems and floral meristems are organized into three cell layers (L1, L2, and L3) with cells in L1 and L2 usually dividing anticlinally (division plane perpendicular to the surface) and cells in L3 dividing in all directions (Poethig 1989; Steeves and Sussex, 1989). Such control of division planes may ensure properly organized meristems and thus proper organ initiation and morphogenesis.

Higher plant cell division exhibits several unique properties: the presence of a preprophase band (PPB), the absence of an obvious microtubule-organizing center (MTOC), and a mechanism for cytokinesis involving vesicle fusion. The division plane in higher plants is first marked in advance by a preprophase band (PPB) of microtubules and actin, which briefly surrounds the cell prior to prophase (Gunning and Wick, 1985) and is not present in animals and fungi. Second, higher plants lack obvious microtubule organizing centers (the centrosome in animals and spindle pole bodies in yeast; Lloyd, 1991; Lambert, 1993). Third, unlike animal cells, where a contractile mechanism is used for cytokinesis (Rappaport, 1986), most higher plants use vesicle fusion for formation of new cell walls and thus for cytokinesis (Pickett-Heaps and Northcote, 1966; Gunning and Wick, 1985). New cell wall and membrane materials are deposited between dividing cells by vesicle fusion via a structure called a phragmoplast. Although the cell division process in higher plants has been well described, little is known about the genes and the control mechanisms underlying the cell division process.

Genetic approaches may be effective in identifying genes

that regulate aspects of cell division. Recently, several genes have been identified and/or isolated that affect plant cytokinesis and preprophase band formation. *KNOLLE* (*KN*; Lukowitz et al., 1996) and *KEULE* (Jürgens et al., 1991) in *Arabidopsis* and *CYD* in pea (Liu et al., 1995) have been shown to be involved in cytokinesis. The *FASS/TON* genes have been implicated in PPB formation (Torres-Ruiz and Jürgens 1994; Traas et al., 1995). The identification, isolation, and analysis of genes in the plant cell division process is beginning to reveal the molecular mechanisms governing cell division, organ development and morphogenesis in higher plants.

In this paper, we report the identification of *tso1*, an *Arabidopsis* mutant that affects proper flower organ development. Our analyses show that *tso1* mutations cause a disorganized floral meristem structure, and *tso1* mutants exhibit similar cellular defects to *kn*, *keule*, and *cyd* mutants. These cellular defects include partially formed cell walls and increased DNA ploidy. Our data suggest that *TSO1* may be similarly involved in cytokinesis. However, unlike *kn*, *keule* and *cyd*, which affect embryos and seedlings, *tso1* mutations only affect later stages of development, mostly limited to flower development. This suggests either that *TSO1* encodes a floral-specific cell division component, or that *TSO1* function is redundant in other tissue types.

MATERIALS AND METHODS

Plant growth and genetics

Plant growth conditions and mutagenesis were described previously (Liu and Meyerowitz, 1995). *tso1-1* was identified in the M₂ generation of an EMS mutagenesis of *ap2-1* mutants in Landsberg *erecta* (Ler) background, and subsequently recovered from its M₂ siblings heterozygous for *tso1-1*. The *ap2-1* mutation was subsequently removed from the *tso1-1* background by back crosses. To map *tso1*, *tso1-1* heterozygous plants were crossed with wild-type plants of

ecotype Columbia (Col). Individual F₂ wild-type plants heterozygous for *tsol-1* were identified by the segregation of *tsol-1* plants in the F₃ generation. One F₃ *tsol-1* plant of each F₂ family was analyzed using SSLP (Simple Sequence Length Polymorphism; Bell and Ecker, 1994) and CAPS (Co-dominant cleaved Amplified Polymorphic Sequences; Konieczny and Ausubel 1993) markers. Linkages to two SSLP markers on chromosome 3 (*nga162* and *nga172*) were found, and the distances between *tsol* and *nga172* and *nga162* are estimated to be 30 and 16 map units respectively. Linkage to a CAPS marker residing in the *SUPERMAN* gene (*SUP*; Sakai et al., 1995) was also detected, and *tsol* was found to be 6 map units north of *SUP*. None of the existing mutations that map to this region of Chromosome 3 exhibits similar phenotypes to *tsol*.

In situ hybridization

Flowers were collected, fixed, embedded, sectioned and hybridized as described previously (Drews et al., 1991).

Confocal microscopy

Samples were collected, fixed, stained and visualized using the procedure of Running et al. (1995).

DNA content measurement

Serial 4 μm sections of floral tissues embedded in JB4 resin (Polysciences Inc.) were stained with 4',6'-diamidino-2-phenylindole (DAPI), and the relative fluorescence units were measured using a MSP 20 microspectrophotometer with digital microprocessor attached to a Zeiss Axiophot microscope equipped with epifluorescence (essentially as described by Friedman, 1991). The area measured was adjusted according to the size of the nucleus, and the background was subtracted each time from an area adjacent to the nucleus measured. The 2C standard was derived by taking an average of readings of several newly divided or dividing nuclei at telophase.

Transmission electron microscopy

Tissues were fixed in 4% paraformaldehyde and 2.5% glutaraldehyde in 25 mM phosphate buffer (pH 7.2-7.4) for 2 hours at room temperature. They were washed, stained en bloc with uranyl acetate (5%), post-fixed in 1% osmium tetroxide, and embedded in LR white resin. 0.08-0.1 μm thick sections were placed on grids, which were stained with lead citrate (33 mg/ml) and uranyl acetate (5%), and visualized using a Philips E420 electron microscope.

RESULTS

TSO1 is required for proper organ formation in flowers

During postembryonic development of *Arabidopsis*, the shoot apical meristem first generates several rosette leaves, then gives rise to cauline leaves with axillary shoots. Subsequently, the apical meristem switches to the production of

flowers instead of cauline leaves, and is then termed an inflorescence meristem. The inflorescence meristem gives rise to floral meristems in a spiral phyllotaxy (Fig. 1A,B), and each floral meristem develops 4 types of floral organs arranged in 4 concentric whorls: 4 sepals in whorl 1, 4 petals in whorl 2, 6 stamens in whorl 3, and 2 fused carpels in whorl 4 (Fig. 1A).

The *tsol-1* mutant was initially identified in an EMS mutagenesis screen by its 'callus-like' flowers (Fig. 1D,G and Methods). In this paper, the term 'callus-like' describes the disorganized cell and organ mass and does not imply extra cell proliferation, nor properties of a callus in plant tissue-culture. The mutation was named 'tso', which means ugly in Chinese. A second EMS-induced allele, *tsol-2*, caused a similar but weaker phenotype. Both *tsol* alleles are recessive to wild type. All subsequent analyses were performed with the strong *tsol-*

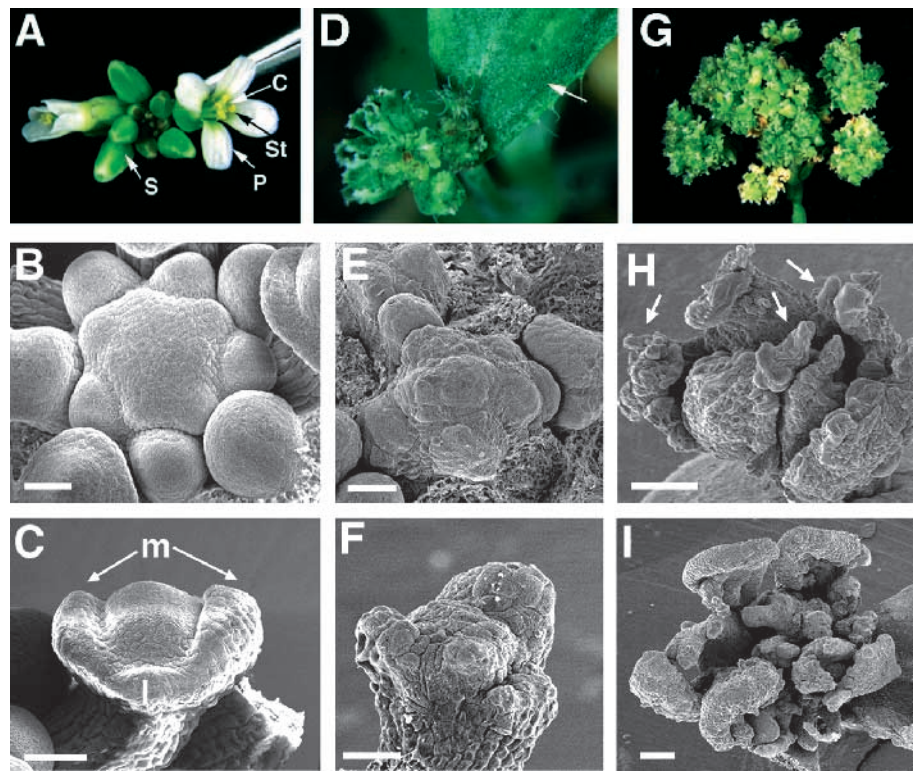


Fig. 1. Wild-type and *tsol-1* plants. (A) A wild-type inflorescence that gives rise to flowers in a spiral pattern. The wild-type flower consists of four organ types: 4 sepals (S) in whorl 1, 4 petals (P) in whorl 2, 6 stamens (St) in whorl 3, and 2 fused carpels (C) in whorl 4. In this picture, the carpels are largely covered by the stamens. (B) A scanning electron microscopy (SEM) picture of a wild-type inflorescence. Floral primordia arise in a spiral pattern. (C) A SEM picture of a wild-type stage 4 flower. The two lateral sepals (l) are situated slightly lower on the pedicel than the two medial sepals (m). (D) A *tsol-1* inflorescence giving rise to many abnormal flowers that lack petals, stamens and carpels. Note the normal morphology of the cauline leaf (arrow). (E) A SEM picture of a *tsol-1* inflorescence meristem. The floral primordia develop in a relatively irregularly spaced spiral pattern. (F) A SEM picture of a stage 4 *tsol-1* flower. The center dome interior to the first whorl sepals is flat, suggesting reduced cell proliferation normally required for interior organ formation. This flower appears to have five sepal primordia, consistent with the presence of 5 to 6 sepals in fully developed *tsol-1* flowers. (G) A fasciated *tsol-1* inflorescence with many more mutant flowers per inflorescence. (H) A SEM picture of a fully developed *tsol-1* flower that exhibits 6 sepals and bloated cells (arrows) on the sepals. (I) A SEM picture of the plate-like (callus-like) organs developing interior to the first whorl sepals of a mature *tsol-1* flower. Occasionally, these plate-like organs exhibit features of petals, stamens, or carpels. Most sepals were removed from this flower. Bar, 20 μm (in B,C,E and F) and 100 μm (in H and I).

I allele. *TSO1* has been mapped to chromosome 3 using PCR-based markers *nga162* (Bell and Ecker, 1994) and *SUPERMAN* (*SUP*; Sakai et al., 1995) and found to be 16 map units south of *nga162* and 6 map units north of *SUP* (see Methods).

Unlike floral homeotic mutations that transform the identity of floral organs (reviewed by Weigel and Meyerowitz, 1994), the *tsol-1* mutation blocks the formation of floral organs in whorls 2, 3 and 4 (Figs 1I, 2E). *tsol* inflorescence occasionally fasciates (Fig. 1G), and the phyllotaxy is also abnormal (compare Fig. 1B with 1E). *tsol-1* mutant flowers develop abnormal sepals (Fig. 1H) but do not develop petals, stamens, or carpels, and are consequently completely sterile (Fig. 1D,G,I). Although sepals are formed in *tsol-1* flowers, they consist of abnormally large and misshapen (bloated) cells (Fig. 1H) and are also abnormal in number; between five to six sepals are formed in each *tsol-1* flower instead of four in wild type (compare Fig. 1A,C with 1F,H).

The *tsol-1* mutant floral meristems were further analyzed using Confocal Laser Scanning Microscopy (CLSM; Fig. 2). Wild-type and *tsol-1* floral meristems were stained with propidium iodide (PI; a DNA staining dye), and then optically sectioned according to the method of Running et al. (1995). In wild type, the three cell layers (L1, L2, and L3) of a floral meristem are distinct and well defined (Fig. 2A), whereas in *tsol-1*, the organization of the three layers appears disrupted (Fig. 2D). In addition, there are fewer cells in *tsol* floral meristems than in wild type (compare Fig. 2A with 2D, and 2B with 2E), and the nuclei in *tsol-1* floral meristems are larger and irregular in shape (Fig. 2D,E), implying a defect in nuclear division. In flowers at stage 6, wild-type floral meristems give rise to organs in the inner whorls via regulated cell division patterns (Fig. 2B). *tsol-1* floral meristems give rise to a few incipient organ primordia (or abnormal outgrowths) in the center of the flowers (Fig. 2E; note the area between the brackets), but not to organ primordia. Cells in these incipient organ primordia are abnormally large and vacuolated; they eventually undergo degeneration, exhibiting degraded cytoplasmic materials (data not shown). Although cellular abnormalities can be detected as early as stage 1 floral meristems, these cellular abnormalities are more frequently detected and more severe in meristems of advanced developmental stages (from stage 2 onward).

The effects of *tsol* mutations are largely

specific to the flowers (Figs 1B, 2). *tsol* plants are largely normal until they start to flower. The tissue-specificity of *tsol-1* mutations was also examined using CLSM. Roots, cauline leaves, apical meristems (including the early vegetative phase

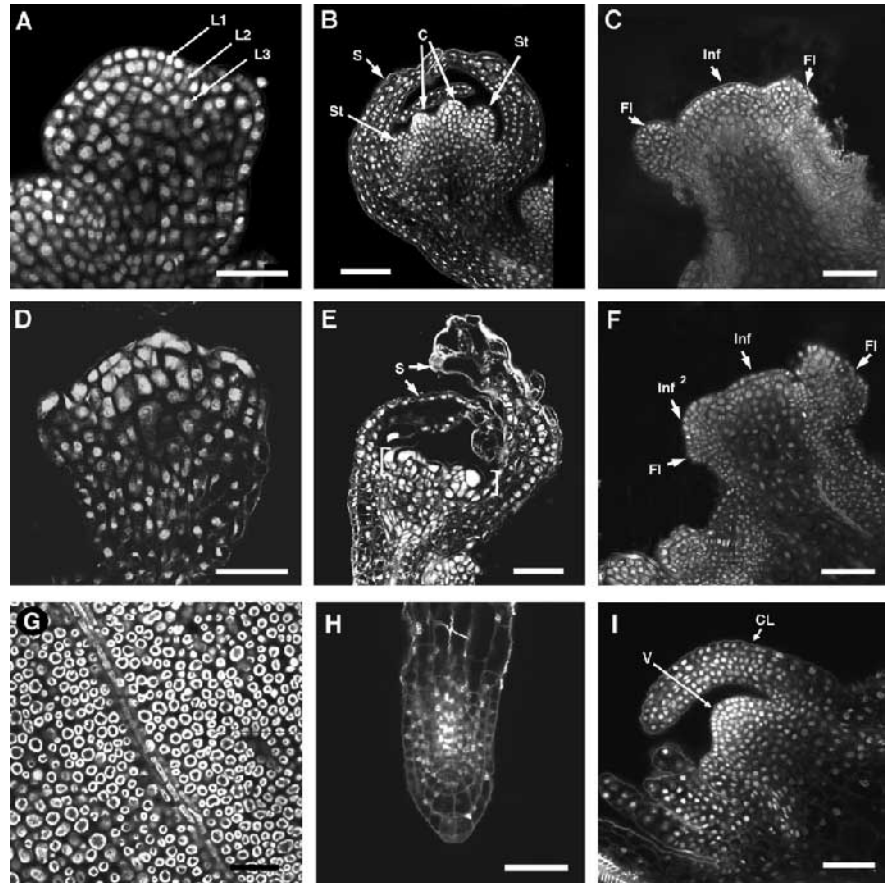


Fig. 2. Confocal microscopy of wild-type and *tsol-1* tissues. Tissues were stained with propidium iodide (PI). Unless specifically noted, all samples shown were optically sectioned in longitudinal axes. Staging of the floral meristems was based on Smyth et al. (1990). S: sepal; St: stamen; C: Carpel; Inf: inflorescence meristem; Inf²: secondary inflorescence meristem; Fl: floral meristem, V: vegetative meristem; CL: cauline leaf. (A) A wild-type stage 3 floral meristem. The three cell layers, L1, L2, and L3, are clearly defined. L1 and L2 are each composed of a single cell layer, whereas L3 consists of several cell layers. (B) A wild-type stage 6 floral meristem with 2 carpel primordia in the center and two stamen primordia flanking the carpels. Petal primordia are still small and not visible in this section. (C) A wild-type inflorescence meristem (Inf), which is flanked by two very young floral meristems (Fl). (D) A *tsol-1* stage 3 floral meristem. The three cell layers are not clearly discernible, and each layer has fewer cells than wild type. The nuclei are irregular in shape and size. (E) A *tsol-1* stage 6 or 7 floral meristem. Shown are two abnormal sepals, interior to which no floral organ develops. Two brackets define the region where cells undergo degeneration (see text). (F) A fasciated *tsol-1* inflorescence meristem (Inf) that is developing a secondary inflorescence meristem (Inf²). A very young floral meristem (stage 1) is developing from the secondary inflorescence meristem. The floral meristem on the right developing from the primary inflorescence is at late stage 2 and is partially damaged by dissection. (G) A paradermal section of a *tsol-1* cauline leaf, showing the chloroplast DNA staining of PI in the parenchyma cells. This image is similar to that of the wild type (not shown). (H) A root tip of a wild-type 7-day seedling germinated on filter paper. Seeds of *tsol-1/+* parents were similarly germinated, and root tips of 55 seedlings (of genotypes: *tsol-1/tsol-1*; *tsol-1/+*, and *+/+*) were examined, all of which were indistinguishable from each other and from those of wild type. (I) A wild-type 12-day old vegetative apical meristem. 23 vegetative apical meristems of genotypes, *tsol-1/tsol-1*; *tsol-1/+*, and *+/+* were examined, all of which were indistinguishable from each other and from those of wild type. Bar, 25 μ m (in A,D,I) and 50 μ m (in B,C,E,F,G,H).

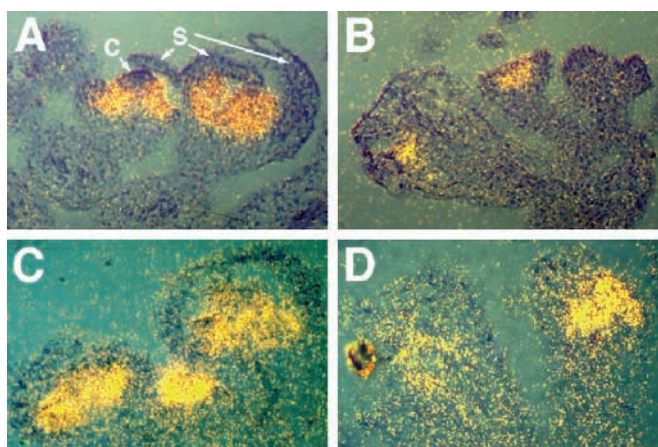


Fig. 3. *AG* and *AP3* RNA expression in wild-type and *tso1-1* flowers. In situ hybridization of an *AG* or *AP3* antisense RNA probe to 8 μ m longitudinal sections of plant inflorescence apices. The tissues were stained with 0.1% toluidine blue. Photos were taken using bright-field and dark-field double exposures with a yellow filter during the dark-field exposure. Yellow grains represent signal. S, sepal; C, carpel. (A) Wild-type flowers. *AP3* RNA is detected in the petal and stamen primordia. (B) *tso1-1* mutant flowers. *AP3* RNA is detected in the region where petals and stamens would arise. The level of RNA expression appears to be reduced relative to wild type. (C) Wild-type flowers. *AG* RNA is detected in the stamen and carpel primordia. (D) *tso1-1* flowers. *AG* RNA is detected in the center of the floral meristems, at what appears to be a lower level than in the wild type.

and later the reproductive phase) were examined in *tso1-1* plants. Although the cauline leaves of *tso1* appear more succulent and slightly darker green than wild type (Figs 1D and 4H), we could not detect any abnormalities or differences from wild type in paradermal sections of *tso1-1* cauline leaves (Fig. 2G). 7 day-old root tips as well as adult roots were also examined; no dramatic differences were observed in the roots of *tso1-1* from those of wild type (Fig. 2H). *tso1-1* vegetative meristems and early inflorescence meristems do not exhibit any discernible defects (Fig. 2I). However, *tso1-1* late inflorescence meristems sometimes fasciate, resulting in enlarged stems, increased numbers of flowers, and abnormal phyllotaxy (Figs 1E,G, 2F). In contrast to the wild-type inflorescence meristem (Fig. 2C), the *tso1-1* primary inflorescence meristem fasciated and bifurcated to produce a secondary inflorescence meristem, from which a floral meristem would develop (Fig. 2F). However, the cellular defects (i.e. abnormal cell layers, enlarged or irregularly shaped nuclei) in *tso1-1* are predominantly found in floral meristems and only rarely in the inflorescence meristems.

***TSO1* functions independently of floral homeotic genes**

To test if the cells in the center of the flower can properly express floral homeotic genes, we examined the expression of the genes *APETALA3* (*AP3*) and *AGAMOUS* (*AG*) (Yanofsky et al., 1990; Jack et al., 1992; reviewed by Weigel and Meyerowitz, 1994). *AP3* is required to specify petal and stamen development, and *AP3* RNA is normally expressed in whorls 2 and 3 of a flower (Fig. 3A). *AG* is required to specify stamen

and carpel development and is normally expressed in whorls 3 and 4 (Fig. 3C). In *tso1-1* mutant flowers, these two genes are expressed in proper domains: *AP3* in an area corresponding to whorls 2 and 3 (Fig. 3B), and *AG* in the center of the floral meristem corresponding to whorls 3 and 4 (Fig. 3D). However, the level of their expression appears to be reduced relative to wild type (Fig. 3B,D). This reduction of floral homeotic gene expression may result from a reduced number of cells and/or reduced transcriptional activities in these cells.

Double mutants homozygous for *tso1* and floral homeotic mutations exhibit additive phenotypes. For example, weak *ap2-1* mutants develop leaves in whorl 1 characterized by branched trichomes (Fig. 4A; Bowman et al., 1991), while strong *ap2-2* mutants develop carpels in whorl 1 characterized by stigmatic tissues and thick carpel walls (Fig. 4D; Bowman et al., 1991). In *ap2-1 tso1-1* double mutants, whorl 1 organs are leaf-like with branched trichomes (Fig. 4B,C), while in *ap2-2 tso1-1* double mutants, whorl 1 organs exhibit carpelloid features such as thick carpel walls and the development of ovule primordia (Fig. 4E,F). Organs interior to the first whorl in either of these double mutants fail to form as in *tso1-1* mutants (Fig. 4B,E). In addition, whorl 1 organs in these double mutants exhibit abnormal cellular morphology such as large and misshapen cells characteristic of *tso1-1* (Fig. 4C,F). Hence, these double mutants express additive phenotypes: the corresponding *ap2* phenotypes in organ identity transformation and the *tso1-1* phenotypes in inner whorl organ formation and in cellular morphology. Since *AP2* normally functions to repress *AG* expression in whorls 1 and 2, the *ap2-2* mutation results in ectopic *AG* expression in whorls 1 and 2 (Bowman et al., 1991; Drews et al., 1991). The carpelloid first whorl organs in the *ap2-2 tso1-1* double mutants suggest that *AG* still functions in the *tso1-1* background, but its function in whorls 2, 3 and 4 is masked by the callus-like defects caused by *tso1-1*. Thus floral homeotic genes and *TSO1* likely act independently of each other.

LEAFY (*LFY*) specifies the identity of floral meristems and, thus, is a member of the meristem identity genes (Weigel et al., 1992). The weak *lfy* mutant, *lfy-5*, enhances the fasciation occasionally observed in *tso1* mutants (Fig. 4G,H,I). The weakly expressed fasciation in *tso1* mutants is significantly enhanced in *lfy-5 tso1-1* double mutants both in the percentage of plants that fasciate and in the extent of fasciation. More cauline leaves and secondary shoots are made in the double mutants than either single mutant, perhaps as a result of fasciation in the shoot apical meristems. Thus, in *lfy5 tso1-1* double mutants, many more leaves are made at the expense of floral tissues (Fig. 4H). Consequently, callus-like tissues are reduced.

***tso1-1* mutant cells possess a high DNA content**

The confocal microscopy analyses indicate that cells in *tso1-1* floral meristems appear to have more highly-stained and larger nuclei, suggesting that *tso1* mutants are defective in nuclear division or cytokinesis, but are capable of DNA synthesis. The DNA content in individual cells was measured through microscopic spectrophotometry. Plastic histological sections of floral tissues were stained with DAPI, and the relative fluorescence units were measured using two different methods. First, nuclei were measured from single 4 μ m sections of wild-type and of *tso1-1* floral meristems. Since the nuclei in wild-type *Arabidopsis* floral meristem cells are, on average, 2-3 μ m in diameter (based on TEM measurements), about half of the nuclei are

encompassed entirely within the 4 µm histological sections. Thus, only large and intact nuclei in each 4 µm were measured. The range of readings are summarized in Fig. 5. While the nuclei of wild-type cells in a stage 5 flower exhibit 2C and 4C values, some of the *tsol-1* nuclei exhibit 8C and even 16C levels of DNA. Since the first method may underestimate certain nuclei that are particularly large and thus may reside in several sections, in the second method, the total fluorescence units of each nucleus were derived by measuring the same nucleus in successive sections to include all nuclear materials. The C value here reflects the combined readings from 2 to 3 successive 4 µm sections. Only those nuclei that are easily traceable in successive sections were measured; thus the readings do not reflect the distribution of C value in the population of cells. While wild-type cells exhibit C values of 2C and 4C, *tsol-1* cells exhibit C values between 2C and 63C. Specifically, C values of 2C, 6C, 6.6C, 9.2C, 10C, 12C, 12.8C, 40C and 63C were found in 16 *tsol-1* nuclei measured using the second method.

Subcellular *tsol-1* defects are associated with cytokinesis

Transmission electron microscopy (TEM) analysis has revealed more details of the subcellular defects in *tsol* floral meristematic cells (Fig. 6). While wild-type floral meristem cells have completely formed cell walls and smooth and round nuclear membranes (Fig. 6A), *tsol* floral meristem cells exhibit a variety of defects. First, cell walls are frequently incompletely formed (Fig. 6C,D,G). We often observed that cell walls project from one side and fail to connect to the other side. Occasionally, cell walls project from both sides and fail to connect to each other. Second, some nuclei are abnormally large, abnormal in shape (Fig. 6B,C,D,E), and the nuclear membrane invaginates and exhibits a wavy (convoluted) shape (Fig. 6D,E; indicated by arrowheads). Cells that exhibit these subcellular defects are more frequently found in the L1 than in the L2 and L3 layers. In L1, 18 of 106 cells or 17%, in L2, 2 of 78 cells or 2.5%, and in L3, 3 of 85 cells or 3.5% exhibited obvious subcellular defects. Abnormal cells are also frequently found in *tsol-1* mutant sepals. Metaphase cells with condensed chromosomes were found in *tsol* floral meristems (Fig. 6F-H), suggesting proper chromosome condensation and nuclear envelope breakdown. However, this may not be true

with all the *tsol* mutant cells. By analysis of serial sections, we observed that the chromosomes in different planes appear to lie in different subcellular locations: at the metaphase plate (Fig. 6F) in one section and near one pole of the cell (Fig. 6G) in another section, suggesting different spindle orientation in different planes of the same cell. Serial sections of cells that appear multinucleate revealed that some of the nuclei are linked by membrane materials (such as the one shown in Fig. 6C). However, in other cases, the multiple nuclei are completely separated from each other, nonetheless remaining in the same cell (data not shown).

DISCUSSION

We have identified and characterized a novel genetic locus, *TSO1*, in *Arabidopsis*. *tsol* mutants are defective in nuclear division (mitosis) and cytokinesis in floral cells. In *tsol* floral

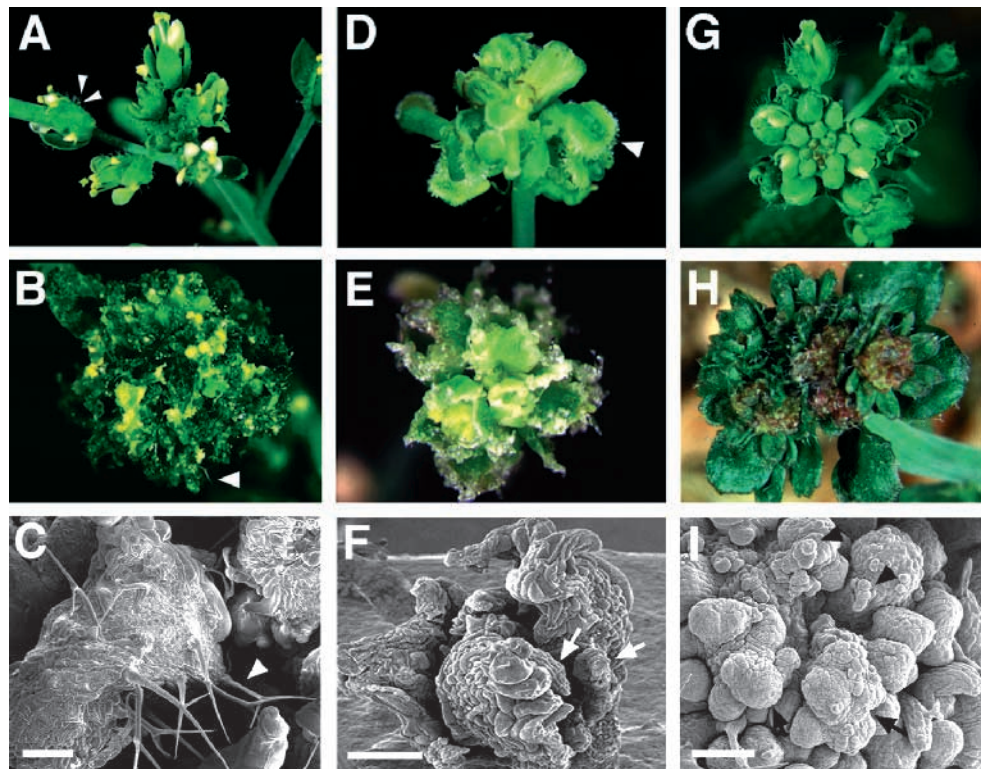


Fig. 4. Double mutants of *tsol ap2* and *tsol lfy*. (A) An *ap2-1* inflorescence. *ap2-1* flowers develop leaves in whorl 1 characterized by branched trichomes (arrow heads). (B) An *ap2-1 tsol-1* inflorescence with flowers that develop leaf-like organs in whorl 1 and callus-like tissues interior to first whorl organs. The arrow head indicates a branched trichome that is characteristic of leaves and is absent from sepals. (C) A close examination of whorl 1 organs in *ap2-1 tsol-1* double mutants by SEM. The arrowhead indicates the branched trichomes that are characteristic of leaves. (D) An *ap2-2* inflorescence. Strong *ap2* mutants such as *ap2-2* develop carpels in whorl 1 with stigmatic tissues (arrow head) and thick carpel walls. (E) An *ap2-2 tsol-1* inflorescence. Flowers exhibit carpelloid whorl 1 organs which are examined in greater detail in F. (F) A SEM photograph of a mature *ap2-2 tsol-1* mutant flower. Abnormal ovule primordia (arrows) are shown, indicating the transformation of whorl 1 organs into carpels. (G) A weak *lfy (lfy-5)* inflorescence. (H) A *lfy-5 tsol-1* inflorescence, which fasciates and bifurcates into many secondary and higher order inflorescences. (I) A more detailed examination of the *lfy-5 tsol-1* fasciated inflorescence meristem by SEM. At least two higher order inflorescence meristems are shown (arrows). Floral organs begin to exhibit abnormal cell morphology as shown by the 'bloated' cells (arrowheads). Bar, 100 µm (C and F) and 50 µm (I).

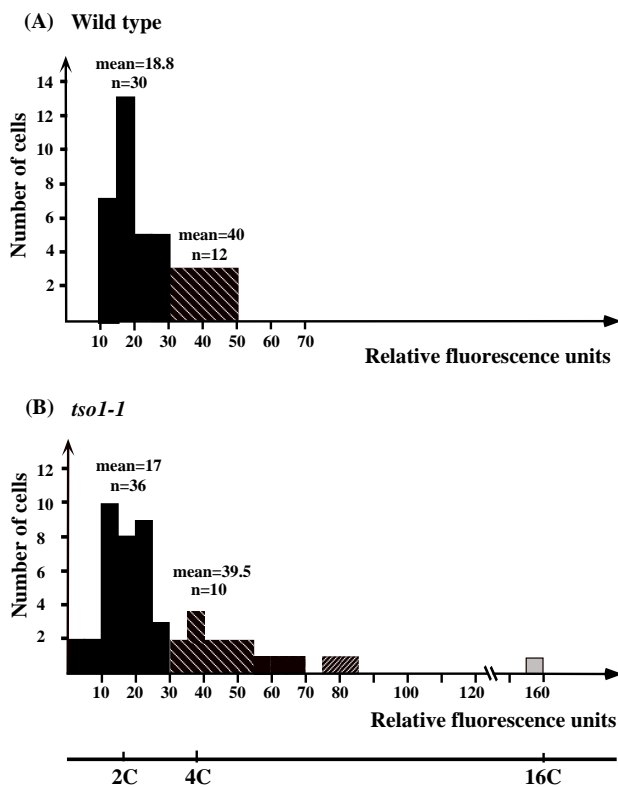


Fig. 5. DNA content in the nuclei of wild-type and *tso1-1* cells. Relative fluorescence units were measured in individual nuclei of 4 μm sections and plotted against the cell number. Those cells that give high C value were mostly positioned interior to sepals as seen in Fig. 2E between the two brackets. Since only certain nuclei in different cell layers (L1, L2 and L3) were measured (see the text), data presented here do not reflect the distribution of C value in the population of cells. n, number of nuclei measured; mean, average fluorescence units. (A) Wild-type floral meristem cells. (B) *tso1-1* floral meristem cells.

meristems and sepals, we observed abnormalities including increased cell size, decreased cell number, disorganized layer structure, increased DNA content per cell, and partially formed cell walls. These defects are different from those of floral homeotic mutants, which act to alter floral organ identity. Based on the additive phenotypes of *tso1* and floral homeotic double mutants, *TSO1* and floral homeotic genes probably act independently of each other.

What is the primary role of *TSO1* in floral meristem cell division? The subcellular phenotypes suggest a defect in mitosis, cytokinesis, and/or failed coordination between mitosis and cytokinesis. These defects can be caused by abnormal cytoskeletal structure, microtubule organizing activity, vesicle fusion during cell plate formation, or failed metaphase/anaphase check points. For instance, incomplete separation of nascent chromosomes could lead to a failure in the formation of two separate nuclei, subsequently blocking completion of cytokinesis. Alternatively, *tso1* mutant cells could fail to monitor the metaphase/anaphase check point, and proceed to cytokinesis without completing mitosis.

The effects of *tso1* mutations are similar to mutants found in the fission yeast *Schizosaccharomyces pombe* (reviewed by Fankhauser and Simanis, 1994) and in other plants (see below). The *S. pombe* mutants *cdc3*, *cdc4*, *cdc8* and *cdc12* arrest as swollen, elongated cells with two or four nuclei, and contain disorganized septal materials. These *S. pombe* genes encode profilin (*cdc3*), a novel form of tropomyosin (*cdc8*), and an EF-hand protein (*cdc4*) (see review by Fankhauser and Simanis, 1994). Another class of *S. pombe* mutations uncouple the normal dependency of mitosis and cytokinesis. This so called *cut* phenotype is seen when cytokinesis occurs despite the fact that nuclear division is blocked, resulting in cleavage of the undivided nucleus by the septum (Uzawa et al., 1990; Samejima et al., 1993). *CUTI* encodes a protein with ATP-binding domains, is a rare component of the insoluble nuclear fraction, and may play a key role in coupling chromosome disjunction with other cell cycle events (Uzawa et al., 1990).

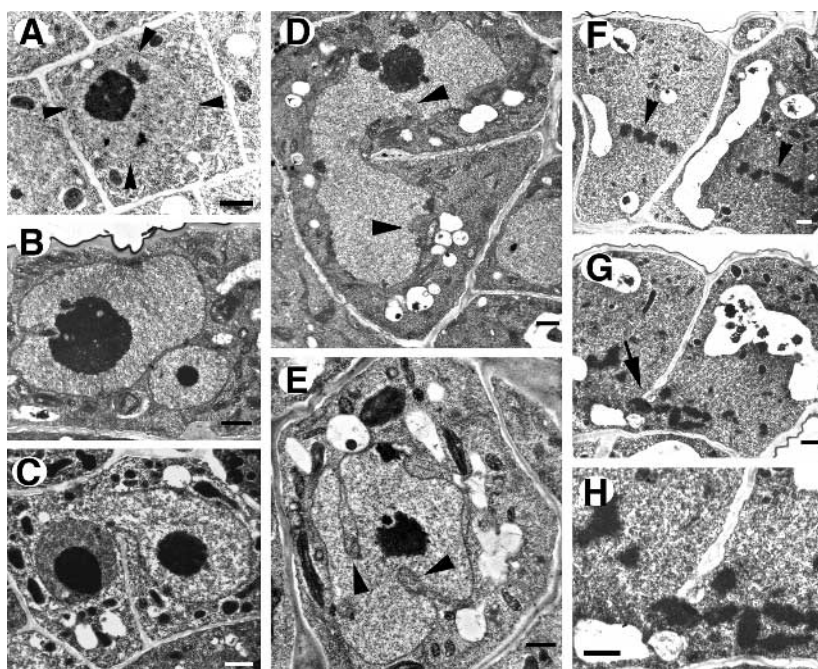


Fig. 6. Transmission electron microscopy of wild-type and *tso1-1* cells. Cells shown are from stage 1 to stage 3 floral meristems. Bar, 1 μm . (A) A wild-type cell. Note the darkly stained nucleolus and the smooth and round nuclear membrane (arrowheads). (B) A single *tso1-1* cell containing two nuclei of different sizes. (C) A single *tso1-1* cell containing two connected nuclei with one nuclear membrane and a partially formed cell wall. The connecting nuclear membrane appears to block the cell wall from connecting to the parental wall on the opposite side. (D) A *tso1-1* cell with an elongated nucleus and a partially formed cell wall. Note the wavy nuclear membrane and nuclear membrane invagination (arrowheads). (E) A *tso1-1* cell showing the invagination of nuclear membranes (arrowheads) and the nuclear pores within the invaginated nuclear membrane. (F) Two *tso1-1* cells at metaphase. The chromosomes (arrowheads) are lying at the metaphase plate. (G) The same two *tso1-1* metaphase cells (in F) in a different section. The chromosomes are gathered near the neck (arrow) of the partial wall. (H) Higher magnification of the neck of the partial wall and the chromosomes as shown in G.

CUT7 encodes kinesin-like protein (Hagan and Yanagida, 1990). The *Arabidopsis* mutants *kn* (Lukowitz et al., 1996), *keule* (Jürgens et al., 1991), and the pea mutant *cyd* (Liu et al., 1995) also exhibit similar subcellular defects to *tsol-1*, including partially formed cell walls, polyploid cells, and multinucleate cells. However, unlike *tsol* mutations, *kn*, *keule*, and *cyd* affect embryos and seedlings. *KN* protein is similar to syntaxins, a protein family involved in vesicular trafficking, implying a role of *KN* in cell plate formation (Lukowitz, et al., 1996). The molecular isolation and analyses of *TSO1* will reveal if *TSO1* shares homology with any of these genes at the molecular level.

In stamen hairs of *Tradescantia*, Ca^{2+} depletion can result in partial cell wall formation (Paul and Goff, 1973; Jürgens, et al. 1994). Similarly, caffeine treatment of plant cells can also mimic this effect (Paul and Goff, 1973; Liu et al., 1995). This is intriguing for Ca^{2+} has long been implicated as a second messenger in both mitosis and cytokinesis. Ca^{2+} has also been implicated in the microtubule organizing center (Lambert, 1993). If similar mechanisms are employed in *Arabidopsis*, *TSO1* could also be involved in regulating intracellular Ca^{2+} concentration and/or Ca^{2+} signal transduction, or it could be a target of caffeine.

In most higher plant cells, new cell plate formation occurs from the center of the dividing cell and then expands outward toward the parental walls. This outward growth of cell walls is achieved by fusion with vesicles containing new cell wall materials. The partially formed cell plates (or wall stubs) observed in *tsol* mutant cells are always attached to parental walls on one side. These cell wall stubs appear to imply an inward cell wall growth. However, the cell wall stubs could also reflect remnants of cell plates that are stabilized by fusion with the parental walls and the unfused cell walls could be rapidly degraded. These cell wall stubs are a common phenomenon, shared among *tsol*, *kn*, *keule*, and *cyd* mutant cells, as well as caffeine-treated plant cells.

Meristem identity genes such as *LFY* and *API* (Irish and Sussex, 1990; Weigel et al., 1992; Bowman, et al., 1993) positively regulate the initiation of the floral program. Thus, any floral tissue-specific genes are directly or indirectly regulated by meristem identity genes even if these floral-specific genes perform diverse functions. Likewise, *TSO1*, as a floral-specific gene, is similarly regulated by the meristem identity genes even though *TSO1* may act in a very different pathway/process from the meristem identity genes. Thus, only if the floral meristem identity is determined and expressed, can the *tsol* mutant effects be manifested.

Two possible mechanisms could be responsible for the largely floral tissue-specific effect of *tsol*: (1) a redundant gene in tissue-types other than flowers or (2) a floral meristem-specific cell division function. In light of the second mechanism, it is likely that different cell division functions may be necessary for different tissue types. For example, floral meristems play fundamental roles for plant reproduction. Mechanisms must exist to ensure proper cell proliferation, meristem architecture, cell-cell communication, organ initiation, differentiation and morphogenesis in the floral meristems. The unique properties of floral meristems may thus require floral-specific cell division regulators or floral-specific components of cell division machineries. Thus further genetic and molecular analyses of *TSO1* may shed light on these

questions regarding tissue-specific cell division control and plant development.

We thank Patrick Koen and Jean Edens for their assistance in TEM, Joshua Levin for the *tsol-2* allele, William Friedman for advice on microscopic spectrophotometric measurements and the use of his facilities, Glen Turner, Michael Chu and Mintao Fan for contributions to double mutant construction, confocal microscopy and mapping respectively. We also thank Eric Baehrecke and members of the Meyerowitz lab for critical reading of the manuscript. Z. L. was a DOE-energy Biosciences Research Fellow of the Life Science Research Foundation, and was previously a post-doctoral fellow of Damon Runyon-Walter Winchell Cancer Research Fund. M. P. R. was a Howard Hughes predoctoral fellow. This work was supported by NIH grant GM 45697 to E. M. M.

REFERENCES

- Bell, C. J. and Ecker, J. R. (1994). Assignment of 30 microsatellite loci to the linkage map of *Arabidopsis*. *Gemonics* **19**, 137-144.
- Bowman, J. L., Smyth, D. R. and Meyerowitz, E. M. (1991). Genetic interactions among floral homeotic genes of *Arabidopsis*. *Development* **112**, 1-20.
- Bowman, J. L., Alvarez, J., Weigel, D., Meyerowitz, E. M. and Smyth, D. R. (1993). Control of flower development in *Arabidopsis thaliana* by *APETALA1* and interacting genes. *Development* **119**, 721-743.
- Drews, G. N., Bowman, J. L. and Meyerowitz, E. M. (1991). Negative regulation of the *Arabidopsis* homeotic gene *AGAMOUS* by the *APETALA2* product. *Cell* **65**, 991-1002.
- Fankhauser, C. and Simanis, V. (1994). Cold fission: Splitting the *pombe* cell at room temperature. *Trends Cell Biol.* **4**, 96-101.
- Friedman, W. E. (1991). Double fertilization in *Ephedra trifurca*, a non-flowering seed plant: the relationship between fertilization events and the cell cycle. *Protoplasma* **165**, 106-120.
- Gunning, B. E. S. and Wick, S. M. (1985). Preprophase bands, phragmoplasts and spatial control of cytokinesis. *J. Cell Sci. Suppl.* **2**, 157-179.
- Hagan, I. and Yanagida, M. (1990). Novel potential mitotic motor protein encoded by the fission yeast *cut7* gene. *Nature* **345**, 81-83.
- Irish, V. F. and Sussex, I. M. (1990). Function of the *apetala-1* gene during *Arabidopsis* floral development. *Plant Cell* **2**, 741-753.
- Jack, T., Brockman, L. L. and Meyerowitz, E. M. (1992). The homeotic gene *APETALA3* of *Arabidopsis thaliana* encodes a MADS box and is expressed in petals and stamens. *Cell* **68**, 683-697.
- Jürgens, G., Mayer, U., Rorres Ruiz, R. A., Berleth, T. and Misera, S. (1991). Genetic analysis of pattern formation in the *Arabidopsis* embryo. *Development Supplement* **1**, 27-38.
- Jürgens, M., Hepler, L. H., Rivers, B. A. and Hepler, P. K. (1994). BAPTA-calcium buffers modulate cell plate formation in stamen hairs of *Tradescantia*: evidence for calcium gradients. *Protoplasma* **183**, 86-99.
- Konieczny, A. and Ausubel, F. M. (1993). A procedure for mapping *Arabidopsis* mutations using codominant ecotype-specific PCR-based markers. *Plant J.* **4**, 403-410.
- Lambert, A. M. (1993). Microtubule organizing centers in higher plants. *Curr. Opin. Cell Biol.* **5**, 116-122.
- Liu, C. M., Johnson, S. and Wang, T. L. (1995). *cyd*, a mutant of pea that alters embryo morphology, is defective in cytokinesis. *Dev. Genet.* **16**, 321-331.
- Liu, Z. and Meyerowitz, E. M. (1995). *LEUNIG* regulates *AGAMOUS* expression in *Arabidopsis* flowers. *Development* **121**, 975-991.
- Lloyd, C. W. (1991). *The Cytoskeletal Basis of Plant Growth and Form* (ed. C. W. Lloyd). London: Academic Press.
- Lukowitz, W., Mayer, U. and Jürgens, G. (1996). Cytokinesis in the *Arabidopsis* embryo involves the syntaxin-related *KNOLLE* gene product. *Cell* **84**, 61-71.
- Paul, D. C. and Goff, C. H. W. (1973). Comparative effects of caffeine, its analogues and calcium deficiency on cytokinesis. *Exp. Cell Res* **78**, 399-413.
- Pickett-Heaps, J. D., and Northcote, D. H. (1966). Organization of microtubules and endoplasmic reticulum during mitosis and cytokinesis in wheat meristems. *J. Cell Sci.* **1**, 109-120.
- Poethig, S. (1989). Genetic mosaic and cell lineage analysis in plants. *Trends Genet.* **5**, 273-277.

- Rappaport, R.** (1986). Establishment of the mechanism of cytokinesis in animal cells. *Int. Rev. Cytol.* **105**, 245-281.
- Running, M. P., Clark, S. E. and Meyerowitz, E. M.** (1995). Confocal microscopy of the shoot apex. In *Methods in Cell Biology: Plant Cell Biology*, Vol 49 (ed. D. W. Galbraith, D. P. Burgue and H. J. Bohnert), pp. 215-227. San Diego: Academic Press.
- Sakai, H., Medrano, L. J. and Meyerowitz, E. M.** (1995). Role of *SUPERMAN* in maintaining *Arabidopsis* floral whorl boundaries. *Nature* **378**, 199-203.
- Samejima, I., Matsumoto, T., Nakaseko, Y., Beach, D. and Yanagida, M.** (1993). Identification of seven new cut genes involved in *Schizosaccharomyces pombe* mitosis. *J. Cell Sci.* **105**, 135-143.
- Smyth, D. R., Bowman, J. L. and Meyerowitz, E. M.** (1990). Early flower development in *Arabidopsis*. *Plant Cell* **2**, 755-767.
- Steeves, T. A. and Sussex, I M.** (1989). *Patterns in Plant Development*. New York: Cambridge University Press, second edition.
- Torres-Ruiz, R. A. and Jürgens, G.** (1994). Mutations in the *fass* gene uncouple pattern formation and morphogenesis in *Arabidopsis* development. *Development* **120**, 2967-2978.
- Traas, J., Bellini, C., Nacry, P., Kronenberger, J., Bouchez, D. and Caboche, M.** (1995). Normal differentiation patterns in plants lacking microtubular preprophase bands. *Nature* **375**, 676-677.
- Uzawa, S., Samejima, I., Hirano, T., Tanaka, K. and Yanagida, M.** (1990). The fission yeast *cut1+* gene regulates spindle pole body duplication and has homology to the budding yeast *ESP1* gene. *Cell* **62**, 913-925.
- Weigel, D., Alvarez, J., Smyth, D.R., Yanofsky, M.F. and Meyerowitz, E.M.** (1992). *LEAFY* controls floral meristem identity in *Arabidopsis*. *Cell* **69**, 843-859.
- Weigel, D. and Meyerowitz, E.M.** (1994). The ABCs of floral homeotic genes. *Cell* **78**, 203-209.
- Yanofsky, M. F., Ma, H., Bowman, J. L., Drews, G. N., Feldmann, K. A. and Meyerowitz, E. M.** (1990). The protein encoded by the *Arabidopsis* homeotic gene *AGAMOUS* resembles transcription factors. *Nature* **346**, 35-40.

(Accepted 29 November 1996)